

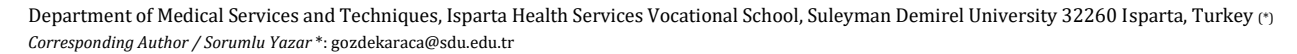
### Dokuz Eylül Üniversitesi Mühendislik Fakültesi Fen ve Mühendislik Dergisi Dokuz Eylul University Faculty of Engineering Journal of Science and Engineering Elektronik/Online ISSN: 2547-958X

RESEARCH ARTICLE / ARAŞTIRMA MAKALESI

## Polydopamine-Nickel Magnetic Micromotors for Efficient Detection of Methylene Blue Dye

Metilen Mavisi Boyasının Etkili Tespiti için Polidopamin-Nikel Manyetik Mikromotorlar

Gözde Yurdabak Karaca 👵



#### Abstract

Rapid industrialization has led to significant environmental challenges, such as the pollution of water bodies by synthetic dyes from industrial waste. These dyes pose health risks, including carcinogenic and mutagenic effects, and contribute to ecological problems. Common dyes like methylene blue (MB), while not highly toxic, can be harmful with prolonged exposure. This study focuses on developing polydopamine-nickel (PDA-Ni) magnetic micromotors for the sensitive detection of MB. These micromotors, produced using an electrochemical template method, can autonomously move and effectively detect high concentrations of MB in aqueous solutions. The tubular structure of the micromotors provides a large surface area for increased adsorption capacity. Electrochemical analyses using cyclic voltammetry show that the micromotors exhibit high sensitivity and stability across a wide range of MB concentrations, with a detection limit of  $0.1~\mu M$ . This study highlights the potential of PDA-Ni micromotors in environmental monitoring and pollutant removal, offering a promising solution for managing water pollution.

Keywords: Micromotor, PDA, Methylene Blue

#### Öz

Hızlı sanayileşme, endüstriyel atıklardan kaynaklanan sentetik boyaların su kütlelerini kirletmesi gibi ciddi çevresel sorunlara neden olmuştur. Bu boyalar, kanserojen ve mutajenik etkiler gibi sağlık riskleri taşır ve ekolojik sorunlara yol açmaktadır. Metilen mavisi (MB) gibi yaygın boyalar, çok toksik olmasa da uzun süreli maruz kalma durumunda zararlı olabilir. Bu çalışma, MB'nin hassas tespiti için Polidopamin-Nikel (PDA-Ni) manyetik mikromotorların geliştirilmesine odaklanmaktadır. Elektrokimyasal şablon yöntemiyle üretilen bu mikromotorlar, kendi kendine hareket ederek sulu çözeltilerde yüksek MB konsantrasyonlarını etkili bir şekilde tespit edebilir. Mikromotorların tübüler yapısı, daha fazla adsorpsiyon kapasitesi için geniş bir yüzey alanı sunar. Döngüsel voltametri ile yapılan analizler, mikromotorların geniş bir MB konsantrasyon aralığında yüksek hassasiyet ve kararlılık gösterdiğini ve 0.1 µM tespit sınırına sahip olduğunu göstermektedir. Bu çalışma, PDA-Ni mikromotorların çevresel izleme ve kirletici gideriminde potansiyelini vurgulamakta ve su kirliliğinin yönetimi için umut verici bir çözüm sunmaktadır.

Anahtar Kelimeler: Mikromotor, PDA, Metilen Mavisi

#### 1. Introduction

Rapid industrialization has brought about a concerning trend—the direct discharge of wastewater laden with synthetic dyes into the environment, presenting a global challenge of significant organic dye contamination in water [1,2]. The health risks associated with synthetic dyes, prevalent in industrial effluents, are substantial. They possess the capacity to induce adverse effects, including cancer and mutagenic impacts on human health [3,4]. Industries spanning textiles, leather, paper, pharmaceuticals, and food contribute to this dilemma by utilizing dyes for product coloring, subsequently discharging untreated effluents into water bodies, thereby exacerbating water pollution[5].

Methylene blue, also known as tetramethylthionine chloride, although generally considered not highly harmful, can pose dangers through continuous exposure, manifesting in symptoms

such as vomiting and an elevated heart rate [5-7]. Notably, methylene blue (MB), a prevalent cationic dve extensively utilized in the dyeing industry, exemplifies the extent of this issue. The detection and removal of dyes from wastewater are crucial for ensuring the safe discharge of treated effluents. Various methods, such as spectrophotometry, chromatography, and fluorimetry, are commonly used to monitor dyes in water samples [8-10]. However, electrochemical techniques are often preferred due to their ease of handling, high selectivity, and sensitivity [11,12]. However, these techniques often face limitations such as high operational costs, complex sample preparation, and the need for sophisticated equipment and trained personnel. Additionally, these methods may lack the sensitivity required to detect low concentrations of dyes, which is critical for early intervention and effective pollution management. To enhance sensitivity, electrodes can be modified with suitable modifiers. Therefore, this work focuses on

modifying electrodes to detect methylene blue (MB) sensitively by using nano/micromotor technology.

Nano/micromotors are structures that can convert various forms of energy into mechanical movement at the micro and nanoscale. Due to their diminutive size, nano/micromotors can demonstrate potential in numerous biomedical and environmental applications, including sensing [13-17], imaging[18], cargo delivery[19,20], microscale manipulation[21,22], biological media exploration, and environmental cleaning and monitoring[23]. Polydopamine (PDA) is inspired by the adhesive proteins found in mussels, which allows it to adhere strongly to a wide variety of surfaces. This strong adhesion ensures that PDAbased sensors and adsorbents remain stable and functional during the detection and removal processes. The robust attachment to substrates prevents the loss of material and maintains the integrity of the sensor or adsorbent over time. PDA contains abundant catechol and amine groups, which facilitate easy functionalization. These functional groups can interact strongly with various pollutants, including methylene blue, through mechanisms such as hydrogen bonding,  $\pi$ - $\pi$  stacking, and electrostatic interactions. This versatility allows PDAs to be tailored for specific applications by incorporating additional functional materials or modifying their surface properties[24]. (PDA) provides a multitude of benefits for detecting and removing methylene blue from water. Its robust adhesive qualities, biocompatibility, ease of customization, large surface area, responsive nature, high adsorption capacity, stability, reusability, and catalytic abilities make it an excellent choice for environmental cleanup applications [25,26]. Incorporating PDA into advanced sensing and adsorption systems shows significant potential for creating effective and sustainable solutions for managing water pollution [27]. Also, magnetic micromotors can exhibit self-propulsion, which enables them to autonomously move through aqueous environments. This self-propulsion ensures a more uniform distribution of the micromotors, leading to more effective and comprehensive pollutant detection [28].

In this study, PDA-Ni magnetic micromotors were prepared using the electrochemical template method and used for the electrochemical determination of methylene blue (MB). This selfpropulsion capability enables the micromotors to navigate through aqueous solutions, reaching and targeting areas with high concentrations of methylene blue. The autonomous motion ensures a more uniform distribution of the micromotors, leading to more effective and comprehensive dye removal. Tubular PDA-Ni-based micromotor structure provides more active sites for the adsorption of methylene blue (MB) molecules, leading to higher adsorption capacities. Nickel imparts magnetic properties to the micromotors, allowing for precise control and manipulation using external magnetic fields. This enables targeted navigation and positioning in complex environments, enhancing the efficiency of pollutant detection and removal. The high surface area ensures that more dye molecules can interact with the micromotor, enhancing the overall efficiency of the detection and removal process.

#### 2. Materials and Methods

#### 2.1. PDA-Ni Magnetic Micromotor Fabrication

The fabrication of tubular-shaped micromotors began with a template-electrodeposition technique as in the previous work [29]. Initially, a silver film was sputtered onto one side of a porous polycarbonate (PC) membrane template, which had pores with a diameter of 2  $\mu$ m and was purchased from Whatman, USA (Catalogue no. 7060-2511)[29]. This was done using RF magnetron sputtering at 50 W and 15 mTorr. The silver-coated

membrane then served as the working electrode in subsequent steps. Aluminum foil was used as the contact for the silver-coated side, while a platinum counter electrode and an Ag/AgCl reference electrode (purchased from CHI) were utilized. PDA-Ni micromotors are created through an electrodeposition process. The outer polydopamine (PDA) layer is electrochemically deposited at +0.9V with a charge of 3C, while the inner magnetic nickel (Ni) layer is deposited at -1.3V with a charge of 13C. Following this, the sputtered silver layer was manually removed from the membrane by polishing it with a 3-4 µm alumina slurry. The membrane was then dissolved in dichloromethane (DCM) for 20 minutes to fully release the microtubes. The released micromotors were collected by centrifugation at 6000 rpm for 5 minutes and thoroughly washed three times with DCM, ethanol, and deionized water (18.2  $M\Omega$  cm at room temperature). Each washing step involved centrifugation for 5 minutes, with three washes performed in total. All obtained micromotors were stored in pure water at room temperature. A Nikon Instrument Inc. Ti Optic LV100ND Model optical microscope was employed to measure and display the speed of the micromotors. Motion videos of the micromotors were recorded at a magnification of 40× and a frame rate of 5 frames per second. An external magnetic field was generated by positioning a coil 6 cm away from the glass slide to magnetically control the PDA-Ni micromotors, with the distance kept constant throughout the experiments. Additionally, each speed measurement was repeated 10 times.

#### 2.2. Electrochemical Analysis

Cyclic voltammetry (CV) analyses were performed using screen-printed carbon electrodes (SPCEs) modified with micromotors. The specific SPCEs used were DropSens DS 110, sourced from Spain. The voltage was scanned between -0.5 V and +1.5 V at a rate of 100 mV/s. The electrolyte solution used in the experiments consisted of 0.1 M KCl, which contained a 5 mM concentration of the Fe(CN) $_6$ <sup>3-</sup>/ $_4$ - redox probe. The modification of the electrodes involved depositing a micromotor dispersion prepared in ethyl alcohol for 15 minutes at room temperature.

#### 2.3. Detection of Methylene Blue

For the detection of organic dyes, the methylene blue organic dye was preferred. The synthesized PDA-Ni magnetic micromotor was incubated with MB organic dye solutions at different concentrations (1x10-8, 1x10-9, 1x10-10, 1x10-11, 1x10-12, 1x10-13, 1x10-14 and 1x10-15 mol/L) for 1 hour each. After the completion of the incubation process, centrifugation was applied to the samples at 6000 rpm for 3 minutes at room temperature. Scheme 1 shows the experimental setup of methylene blue detection by using PDA-Ni micromotor.

Methylene Blue Solution

# N S CI

SPCE

Scheme 1. Experimental Setup

PDA-Ni micromotor

#### 3. Results and Dicussion

Figure 1 shows SEM images and analyses confirm the successful synthesis and structural integrity of the PDA-Ni micromotors. Figure 1a shows a side view of the tubular PDA-Ni micromotor, measuring approximately 9.052 µm in length. This tubular structure is crucial for providing a high surface area, which enhances the adsorption capacity for methylene blue molecules. Figure 1b presents a top view of the micromotor, with an inner diameter of about 1.109 µm. This view highlights the hollow nature of the micromotor, which is essential for its selfpropulsion and effective distribution in aqueous solutions. Figure 1c displays the Energy Dispersive X-ray Spectroscopy (EDS) results, confirming the elemental composition of the micromotor. The presence of carbon (C), oxygen (O), and nickel (Ni) is consistent with the PDA-Ni structure, indicating successful fabrication. The high nickel content is particularly important for the magnetic properties that enable controlled movement in the presence of an external magnetic field.

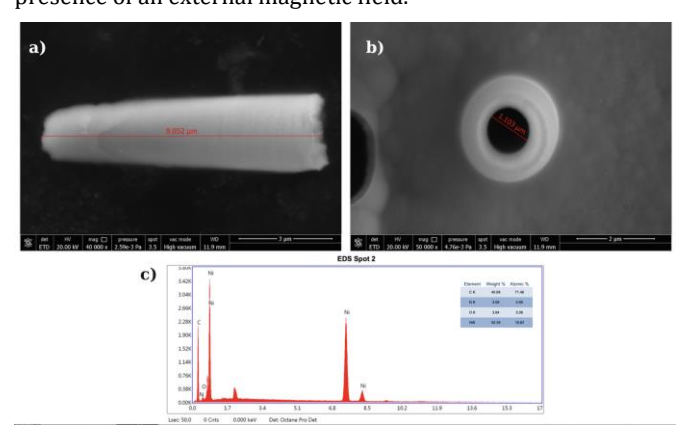


**Figure 1.** a) Side view of PDA-Ni micromotor b) Top view of PDA-Ni micromotor c) EDS results of PDA-Ni micromotor

Figure 2 illustrates the speed of PDA-Ni micromotors under different conditions. The micromotors exhibit higher speeds under magnetic and combined magnetic + Near-infrared (NIR) conditions compared to NIR alone, demonstrating the effectiveness of magnetic control in enhancing micromotor propulsion. The micromotors achieve a speed of approximately  $25 \,\mu\text{m/s}$  when only a magnetic field is applied. This indicates that the magnetic properties of the nickel layer effectively enhance the propulsion of the micromotors. Under NIR conditions alone, the speed drops significantly to around 5 µm/s. When exposed to light, the asymmetric nanobowl structure of PDA exhibits a high photothermal conversion efficiency. This capability generates an uneven thermal gradient field, which in turn leads to selfthermophoretic movement [28]. When both magnetic and NIR conditions are applied, the speed increases to about 30  $\mu$ m/s. This demonstrates a synergistic effect, where the combination of magnetic and NIR stimuli results in the highest propulsion speed. The experimental findings show that the use of a magnetic field and NIR light can effectively control the speed, direction, and position of the micromotors remotely [28,30].

PDA micromotor, incubated with MB dye at 8 different concentrations, underwent photocatalytic reactions resulting from 1 minute of NIR exposure. The cyclic voltammetry (CV) graphs for the degradation of the dye at scanning rates of 5, 10, 25, 50, 75 and 100 mV/s are presented in Figure 3.

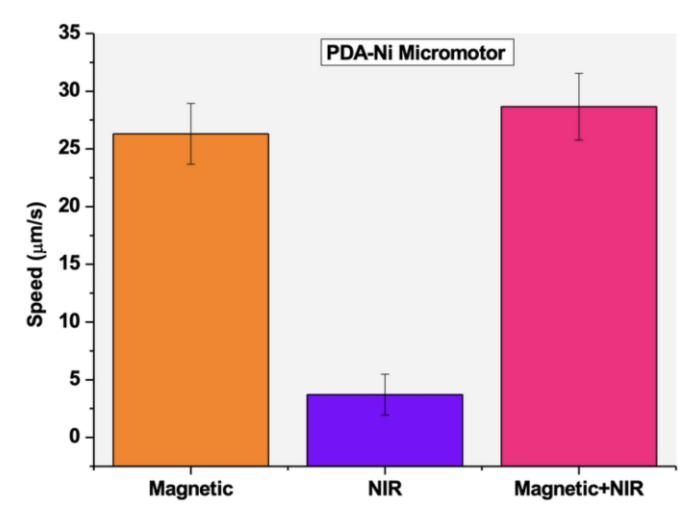
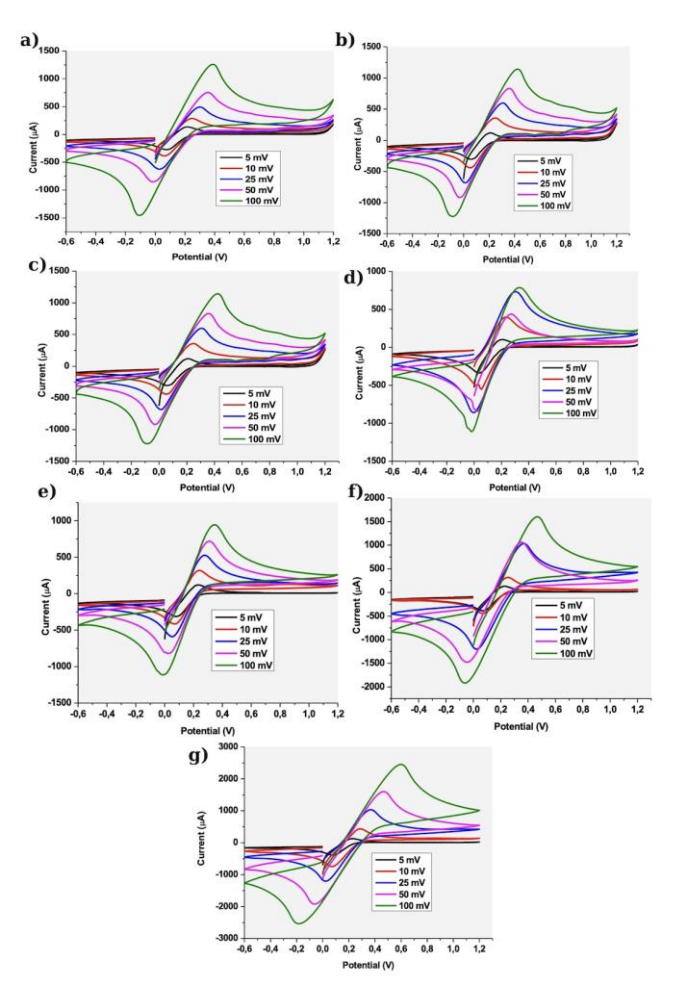


Figure 2. Micromotor speed due to magnetic field and NIR light source



**Figure 3.** Different Concentration of MB incubated micromotor CV results with different scan rates (5 mV/s, 10 mV/s, 25 mV/s, 50 mV/s, 100 mV/s) a)  $10^{-6}$  M b)  $10^{-7}$  M c)  $10^{-8}$  M d) $10^{-9}$  M e) $10^{-10}$  M f)  $10^{-11}$  M g) $10^{-12}$  M

Each subfigure (Figure 3a to 3g) corresponds to a specific concentration of MB, ranging from  $10^{-6}$  M to  $10^{-12}$  M. According to the provided graphs, a clear increase in current values is observed as the scanning rate increases. This indicates that the electrochemical response of the micromotors is dependent on the scan rate, which is typical in CV analyses as higher scan rates can enhance the peak currents due to faster electron transfer kinetics [31,32]. The current increase observed in the CV results as the concentration of MB decreases can be attributed to the enhanced electrochemical activity of the PDA-Ni micromotors at lower concentrations ( $10^{-11}$ M (Figure 3f) and  $10^{-12}$ M (Figure 3g)). This phenomenon is likely due to the increased availability of active sites on the micromotors for interaction with MB molecules when the concentration is lower. As the concentration decreases, the micromotors can more effectively adsorb and degrade the MB,

leading to a more pronounced electrochemical response. This is reflected in the CV graphs, where the current values increase as the concentration of MB decreases, indicating that the micromotors maintain high sensitivity and efficiency even at lower levels of the dye. This behavior underscores the potential of PDA-Ni micromotors for applications requiring the detection and removal of low concentrations of pollutants in environmental settings.

Figure 4 presents the cyclic voltammetry (CV) results for PDA-Ni micromotors incubated with methylene blue (MB) at various concentrations, specifically focusing on their stability over 20 cycles at a scan rate of 100 mV/s. Each subfigure (Figure 4a to 4g) corresponds to a specific concentration of MB, ranging from  $10^{-6}$  M to  $10^{-12}$  M.

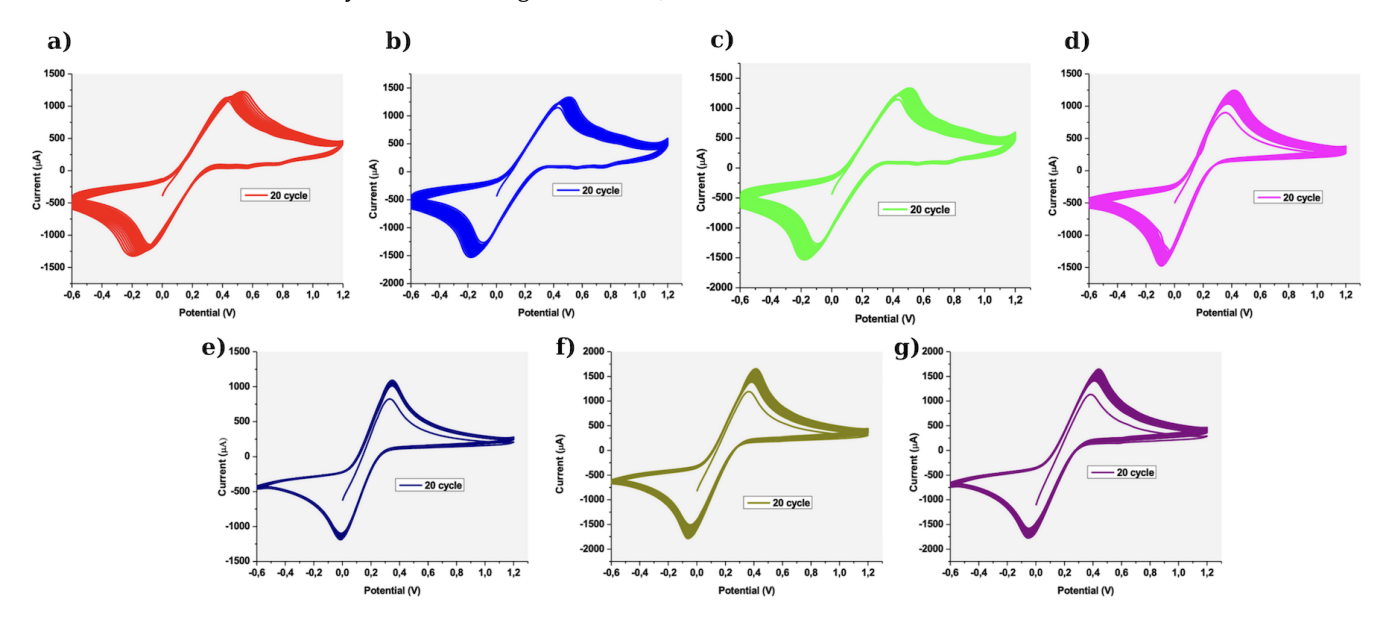


Figure 4. Different Concentrations of MB incubated micromotor stability for 20 cycle CV results with 100 mV/s scan rate a)  $10^{-6}$  M b)  $10^{-7}$  M c)  $10^{-8}$  M d) $10^{-9}$ M e) $10^{-10}$  M f)  $10^{-11}$  M g) $10^{-12}$  M

In Figure 4a, the higher concentration of MB, the CV results show relatively stable current values over the 20 cycles, indicating that the micromotors maintain their electrochemical activity without significant degradation or loss of performance. Like Figure 4a, Figure 4b shows the micromotors exhibit stable performance over 20 cycles, with consistent peak currents. Figure 4c continues to show stable current values, although there might be slight variations in peak currents compared to higher concentrations. At  $10^{-9}\,\mathrm{M}$  concentration (Figure 4d), the micromotors maintain stable electrochemical activity, with consistent peak currents over the cycles. Figure 4e and Figure 4f show the consistent current values across the cycles. At the lowest concentration tested (Figure 4g), the micromotors still maintain stable electrochemical activity, with consistent peak currents. his highlights the exceptional sensitivity of the PDA-Ni micromotors, capable of detecting and interacting with very low concentrations of MB, making them suitable for applications in detecting trace levels of pollutants. Overall, Figure 4 demonstrates the stability and robustness of PDA-Ni micromotors across a range of MB concentrations, showcasing their potential for reliable and repeated use in environmental monitoring and pollutant detection applications.

Figure 5 shows a cyclic voltammetry (CV) graph (Figure 5a) and a calibration curve (Figure 5b) for different concentrations of

methylene blue (MB) dye incubated PDA-Ni micromotors. The CV graph illustrates the electrochemical response of PDA-Ni micromotors when incubated with various concentrations of MB dye. The scan rate used for these measurements is 100 mV/s.

The graph shows distinct peaks corresponding to the redox reactions of MB at different concentrations, ranging from higher to lower levels. As the concentration of MB decreases, the peak current values increase, indicating enhanced electrochemical activity at lower concentrations. This suggests that the micromotors have a higher sensitivity and efficiency in detecting and interacting with MB molecules when present in lower amounts. The graph demonstrates the capability of PDA-Ni micromotors to maintain a strong electrochemical response across a wide range of MB concentrations, highlighting their potential for detecting low levels of pollutants in environmental applications. The calibration curve (Figure 5b) is derived from the peak current values obtained in the CV graph (Figure 5a) plotted against the corresponding concentrations of MB dye. The Limit of Detection (LOD) calculated from Figure 5b for the PDA-Ni micromotors detecting methylene blue is  $0.1~\mu\text{M}$ , demonstrating their high sensitivity and capability to detect low concentrations of the dye.

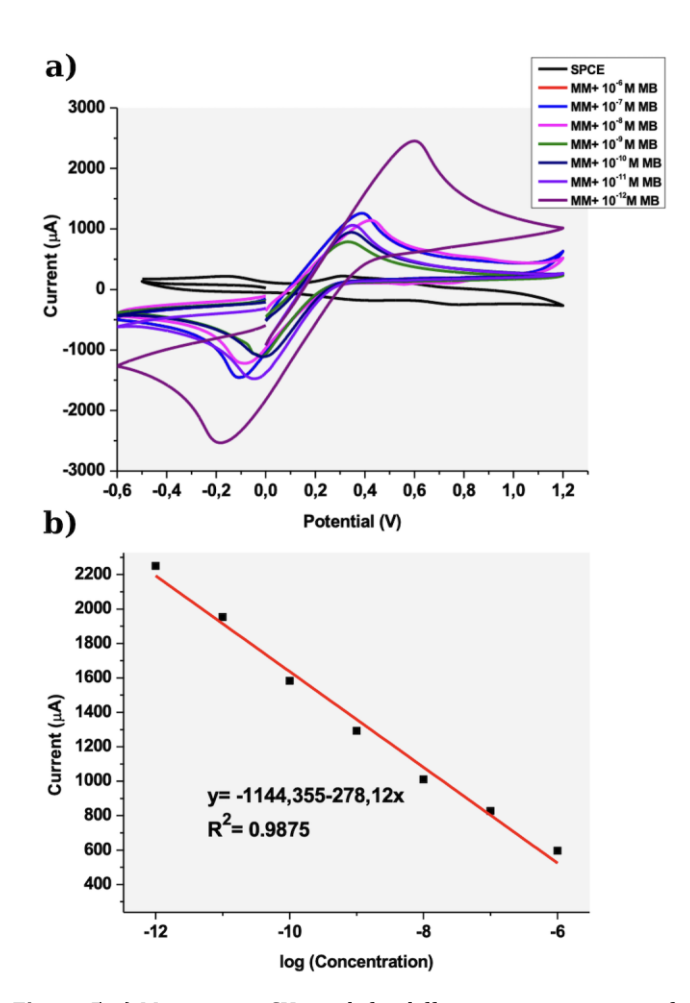


**Figure 5**. a) Micromotor CV graph for different concentrations of MB dye (scan rate: 100 mV/s) b) calibration curve

#### 4. Conclusions

In conclusion, this study successfully demonstrates the potential of polydopamine-nickel (PDA-Ni) magnetic micromotors in addressing the critical issue of water pollution caused by synthetic dyes, particularly methylene blue (MB). The innovative of PDA-Ni micromotors, fabricated through electrochemical template method, showcases their ability to effectively detect MB. The micromotors' self-propulsion capabilities and high surface area significantly enhance their adsorption capacity, making them highly efficient in targeting and eliminating dye pollutants. 'The study on polydopamine-nickel (PDA-Ni) magnetic micromotors highlights their significant advantages over existing dye detection technologies. These micromotors, fabricated using an electrochemical template method, exhibit self-propulsion capabilities that allow them to navigate and target high concentrations of methylene blue (MB) in aqueous solutions effectively. Unlike traditional methods such as spectrophotometry and chromatography, which require complex equipment and sample preparation, PDA-Ni micromotors offer a more straightforward and cost-effective approach. Electrochemical analyses, specifically cyclic voltammetry, confirm micromotors' high sensitivity and stability across a wide range of MB concentrations, achieving a detection limit of 0.1 µM. These findings highlight the promising application of PDA-Ni micromotors in environmental monitoring, offering a sustainable and effective solution for mitigating the adverse impacts of industrial effluents on water bodies. The study paves the way for further exploration and development of advanced micromotor technologies for environmental cleanup and protection.

#### Ethics committee approval and conflict of interest statement

This article does not require ethics committee approval. This article has no conflicts of interest with any individual or institution.

#### References

- Li, X., Zhao, Y., Wang, D., Du, X. 2023. Dual-propelled PDA@MnO2 nanomotors with NIR light and H2O2 for effective removal of heavy metal and organic dye, Colloids and Surfaces A: Physicochemical and Engineering Aspects, Vol. 658, p.130712. DOI: 10.1016/j.colsurfa.2022.130712
- [2] Hu, X., Yang, Y., Wang, W., Wang, Y., Gong, X., Geng, C., Tang, J. 2023. Hollow Fe3+-Doped Anatase Titanium Dioxide Nanosphere for Photocatalytic Degradation of Organic Dyes, ACS Applied Nano Materials, Vol. 6, pp.18999–19009. DOI: 10.1021/acsanm.3c03452
- [3] Fadillah, G., Saleh, T.A., Wahyuningsih, S., Ninda Karlina Putri, E., Febrianastuti, S. 2019. Electrochemical removal of methylene blue using alginate-modified graphene adsorbents, Chemical Engineering Journal, Vol. 378, p.122140. DOI: 10.1016/j.cej.2019.122140
- [4] Ibupoto, A.S., Qureshi, U.A., Ahmed, F., Khatri, Z., Khatri, M., Maqsood, M., Brohi, R.Z., Kim, I.S. 2018. Reusable carbon nanofibers for efficient removal of methylene blue from aqueous solution, Chemical Engineering Research and Design, Vol. 136, pp.744–752. DOI: 10.1016/j.cherd.2018.06.035
- [5] Hayat, M., Shah, A., Nisar, J., Shah, I., Haleem, A., Ashiq, M.N. 2022. A Novel Electrochemical Sensing Platform for the Sensitive Detection and Degradation Monitoring of Methylene Blue, Catalysts, Vol. 12, p.306. DOI: 10.3390/catal12030306
- [6] Obayomi, K.S., Lau, S.Y., Zahir, A., Meunier, L., Jianhua, Z., Dada, A.O., Rahman, M.M. 2023. Removing methylene blue from water: A study of sorption effectiveness onto nanoparticles-doped activated carbon, Chemosphere, Vol. 313, p.137533. DOI: 10.1016/j.chemosphere.2022.137533
- [7] Zhao, Y., Wang, D., Luan, Y., Du, X. 2022. NIR-light propelled bowl-like mesoporous polydopamine@UiO-66 metal-organic framework nanomotors for enhanced removal of organic contaminant, Materials Today Sustainability, Vol. 18, p.100129. DOI: 10.1016/j.msust.2022.100129
  [8] Tang, B., Xi, C., Zou, Y., Wang, G., Li, X., Zhang, L., Chen, D., Zhang, J. 2014.
- [8] Tang, B., Xi, C., Zou, Y., Wang, G., Li, X., Zhang, L., Chen, D., Zhang, J. 2014. Simultaneous determination of 16 synthetic colorants in hotpot condiment by high performance liquid chromatography, Journal of Chromatography B, Vol. 960, pp.87– 91. DOI: 10.1016/j.jchromb.2014.04.026
- [9] Alesso, M., Bondioli, G., Talío, M.C., Luconi, M.O., Fernández, L.P. 2012. Micelles mediated separation fluorimetric methodology for Rhodamine B determination in condiments, snacks and candies, Food Chemistry, Vol. 134, pp.513–517. DOI: 10.1016/j.foodchem.2012.02.110
- [10] Zhu, X., Liu, J., Zhang, Z., Lu, N., Yuan, X., Wu, D. 2015. Green synthesis of a bromocresol purple/graphene composite and its application in electrochemical determination of 2,4,6-trichlorophenol, Analytical Methods, Vol. 7, pp.3178–3184. DOI: 10.1039/C5AY00177C
- [11] Terbouche, A., Lameche, S., Ait-Ramdane-Terbouche, C., Guerniche, D., Lerari, D., Bachari, K., Hauchard, D. 2016. A new electrochemical sensor based on carbon paste electrode/Ru(III) complex for determination of nitrite: Electrochemical impedance and cyclic voltammetry measurements, Measurement, Vol. 92, pp.524–533. DOI: 10.1016/j.measurement.2016.06.034
- [12] Yadav, S., Carrascosa, L.G., Sina, A.A.I., Shiddiky, M.J.A., Hill, M.M., Trau, M. 2016. Electrochemical detection of protein glycosylation using lectin and protein-gold affinity interactions, Analyst, Vol. 141, pp.2356–2361. DOI: 10.1039/C6AN00528D
- [13] Zhang, Y., Yuan, K., Zhang, L. 2019. Micro/Nanomachines: from Functionalization to Sensing and Removal, Advanced Materials Technologies, Vol. 4, p.1800636. DOI: 10.1002/admt.201800636
- [14] Kim, K., Guo, J., Liang, Z., Fan, D. 2018. Artificial Micro/Nanomachines for Bioapplications: Biochemical Delivery and Diagnostic Sensing, Advanced Functional Materials, Vol. 28, p.1705867. DOI: 10.1002/adfm.201705867
- [15] Zhang, X., Chen, C., Wu, J., Ju, H. 2019. Bubble-Propelled Jellyfish-like Micromotors for DNA Sensing, ACS Applied Materials & Interfaces, Vol. 11, pp.13581–13588. DOI: 10.1021/acsami.9b00605
- [16] Esteban-Fernández de Ávila, B., Martín, A., Soto, F., Lopez-Ramirez, M.A., Campuzano, S., Vásquez-Machado, G.M., Gao, W., Zhang, L., Wang, J. 2015. Single Cell Real-Time miRNAs Sensing Based on Nanomotors, ACS Nano, Vol. 9, pp.6756–6764. DOI: 10.1021/acsnano.5b02807
- [17] Celik Cogal, G., Das, P.K., Yurdabak Karaca, G., Bhethanabotla, V.R., Uygun Oksuz, A. 2021. Fluorescence Detection of miRNA-21 Using Au/Pt Bimetallic Tubular Micromotors Driven by Chemical and Surface Acoustic Wave Forces, ACS Applied Bio Materials, Vol. 4, pp.7932-7941. DOI: 10.1021/acsabm.1c00854
- [18] Gao, C., Wang, Y., Ye, Z., Lin, Z., Ma, X., He, Q. 2021. Biomedical Micro-/Nanomotors: From Overcoming Biological Barriers to In Vivo Imaging, Advanced Materials, Vol. 33, p.2000512. DOI: 10.1002/adma.202000512
- [19] Mena-Giraldo, P., Orozco, J. 2021. Polymeric micro/nanocarriers and motors for cargo transport and phototriggered delivery, Polymers, Vol. 13, p.3920. DOI: 10.3390/polym13223920
- [20] Gao, W., Kagan, D., Pak, O.S., Clawson, C., Campuzano, S., Chuluun-Erdene, E., Shipton, E., Fullerton, E.E., Zhang, L., Lauga, E., Wang, J. 2012. Cargo-towing fuel-free magnetic nanoswimmers for targeted drug delivery, Small, Vol. 8, pp.460–467. DOI: 10.1002/smll.201101909
- [21] Liu, L., Chen, B., Liu, K., Gao, J., Ye, Y., Wang, Z., Qin, N., Wilson, D.A., Tu, Y., Peng, F. 2020. Wireless Manipulation of Magnetic/Piezoelectric Micromotors for Precise Neural Stem-Like Cell Stimulation, Advanced Functional Materials, Vol. 30, p.1910108. DOI: 10.1002/adfm.201910108

- [22] Burdick, J., Laocharoensuk, R., Wheat, P.M., Posner, J.D., Wang, J. 2008. Synthetic nanomotors in microchannel networks: Directional microchip motion and controlled manipulation of cargo, Journal of the American Chemical Society, Vol. 130, pp.8164–8165. DOI: 10.1021/j.a803529u
- [23] Jurado-Sánchez, B., Wang, J. 2018. Micromotors for environmental applications: a review, Environmental Science: Nano, Vol. 5, pp.1530–1544. DOI: 10.1039/c8en00299a
- [24] Chen, R., Lin, B., Luo, R. 2022. Recent progress in polydopamine-based composites for the adsorption and degradation of industrial wastewater treatment, Heliyon, Vol. 8, p.e12105. DOI: 10.1016/j.heliyon.2022.e12105
- [25] Zeng, Q., Lin, H., Qu, Y., Huang, Z., Kong, N., Han, L., Chen, C., Li, B., Teng, J., Xu, Y., Shen, L. 2023. Breaking the cost barrier: polydopamine@NixCo100-x nanotubes as efficient photocatalysts for organic pollutant degradation, Journal of Cleaner Production, Vol. 415, p.137910. DOI: 10.1016/j.jclepro.2023.137910
- [26] Kesornsit, S., Jitjankarn, P., Sajomsang, W., Gonil, P., Bremner, J.B., Chairat, M. 2019. Polydopamine-coated silk yarn for improving the light fastness of natural dyes, Coloration Technology, Vol. 135, pp.143–151. DOI: 10.1111/cote.12390
- [27] Li, H., Yin, D., Li, W., Tang, Q., Zou, L., Peng, Q. 2021. Polydopamine-based nanomaterials and their potentials in advanced drug delivery and therapy, Colloids and Surfaces B: Biointerfaces, Vol. 199, p.111502. DOI: 10.1016/j.colsurfb.2020.111502
- [28] Turker, A., Yurdabak Karaca, G. 2024. Dual motion principal Au-Ni-PDA-CuS micromotors with NIR light and magnetic effect for detection of organic dye, Microchemical Journal, Vol. 207, p.111701. DOI: 10.1016/j.microc.2024.111701
- [29] Kara, U., Kilicoglu, O., Turker, A., Yurdabak Karaca, G. 2025. Multifunctional nano/micromotors: design, characterization, and potential applications in radiation attenuation, Radiation Effects and Defects in Solids, Vol. 2025, pp.1–16. DOI: 10.1080/10420150.2025.2467364
- [30] Jiang, W., Ye, G., Chen, B., Liu, H. 2021. A dual-driven biomimetic microrobot based on optical and magnetic propulsion, Journal of Micromechanics and Microengineering, Vol. 31, p.035003. DOI: 10.1088/1361-6439/abd8de
- [31] Pu, X., Zhao, D., Fu, C., Chen, Z., Cao, S., Wang, C., Cao, Y. 2021. Understanding and Calibration of Charge Storage Mechanism in Cyclic Voltammetry Curves, Angewandte Chemie International Edition, Vol. 60, pp.21310–21318. DOI: 10.1002/anie.202104167
- [32] Randviir, E.P. 2018. A cross examination of electron transfer rate constants for carbon screen-printed electrodes using Electrochemical Impedance Spectroscopy and cyclic voltammetry, Electrochimica Acta, Vol. 286, pp.179–186. DOI: 10.1016/j.electacta.2018.08.021